Eur. J. Mineral.
2009, **21**, 1287–1300
Published online December 2009

UH*P* metamorphic evolution of coesite-bearing eclogite from the Yuka terrane, North Qaidam UH*P*M belt, NW China

GUIBIN ZHANG[1,2], DAVID J. ELLIS[2], ANDREW G. CHRISTY[2], LIFEI ZHANG[1,*], YAOLING NIU[3] and SHUGUANG SONG[1]

[1] MOE Key Laboratory of Orogenic Belts and Crustal Evolution, School of Earth and Space Sciences, Peking University, Beijing 100871, China
*Corresponding author, e-mail: lfzhang@pku.edu.cn
[2] Research School of Earth Sciences, The Australian National University, Canberra ACT 0200, Australia
[3] Department of Earth Sciences, Durham University, Durham, DH1 3LE, UK

Abstract: Coesite, recognized petrographically and confirmed by Raman spectroscopy, is reported from a coarse-grained eclogite from the Yuka terrane, North Qaidam UH*P* metamorphic belt. This represents the first record of UH*P* metamorphism in the western part of this belt. In addition, inclusions of Ab + Qtz assemblage in garnet with strong evidence for volume expansion may have derived from a Jd + Coe precursor. Two types of eclogite, coarse-grained and fine-grained, are exposed in the Yuka terrane. The eclogites experienced three distinguishable metamorphic stages: (1) a pre-peak metamorphic stage recorded by the mineral assemblage of Amp + Pl + Qtz in the garnet core at P = 0.8-1.0 GPa, T = 450–560 °C for the coarse-grained eclogite and P = 1.0–1.2 GPa, T = 450–510 °C for the fine-grained eclogite, and by the mineral assemblage of Cpx + Phn in the garnet mantle at P = 2.25–2.65 GPa, T = 550–610 °C for the coarse-grained eclogite; (2) the peak stage characterized by the mineral assemblage of Grt + Omp + Phn + Qtz/Coe + Rt at P = 3.0 GPa, T = 652 °C for the coarse-grained eclogite, and Grt + Omp + Phn + Rt + Qtz at P = 2.9–3.2 GPa, T = 566–613 °C for the fine-grained eclogite; and (3) a retrograde stage recorded by the garnet reaction rims, the breakdown of omphacite, and the pervasive retrograde mineral assemblage of Grt + Amp + Pl + Qtz at P = 0.7–1.1 GPa, T = 550–590 °C for the coarse-grained eclogite. The coesite inclusion and the calculated *P-T* paths suggest that the Yuka UH*P*M terrane experienced fast and deep subduction (~100 km) under a cool geothermal gradient (6–7 °C/km) followed by rapid exhumation.

Key-words: coesite inclusion, Ab + Qtz, eclogite, P-T path, Yuka terrane, North Qaidam UH*P* metamorphic belt, NW China.

1. Introduction

The discovery and tectonic implications of ultra-high pressure metamorphic (UH*P*M) coesite (*e.g.*, Song, 2001; Yang *et al.*, 2001; Song *et al.*, 2003a) from zircons in paragneisses from the eastern part of the North Qaidam UH*P*M belt has been the subject of considerable interest in recent years. The North Qaidam metamorphic belt is a product of continental subduction/collision in the Paleozoic (Yang *et al.*, 2001; Song *et al.*, 2003b, 2006; Zhang *et al.*, 2008). In comparison with other Chinese UH*P*M terrains, the metamorphic mineral assemblages of the North Qaidam belt resemble those of Dabie-Sulu (Jahn, 1999; Liou & Zhang, 2002; Zheng *et al.*, 2003; Liou *et al.*, 2004), and differ greatly from those of Tianshan (Zhang *et al.*, 2002a and b, 2007).

Coesite, a diagnostic indicator of UH*P*M, was first found in eclogite and its host paragneisses from the eastern end (*e.g.*, Dulan terrane and Shaliuhe cross section) of the North Qaidam belt (Yang *et al.*, 2001; Song *et al.*, 2003a; Zhang *et al.*, 2009a and b). Some previous studies have proposed that the Altun metamorphic terrane is the western extension of the North Qaidam UH*P*M belt (Liu *et al.*, 1999; Zhang *et al.*, 2001, 2005; Mattinson *et al.*, 2007). Although diamond as inclusions in zircons has been found from Luliangshan UH*P* garnet peridotite (Song *et al.*, 2005b) in the western part of the North Qaidam belt (*e.g.*, Xitieshan, Luliangshan and Yuka terrane; see Fig. 1), there has been no confirmation from the eclogites on the UH*P*M conditions other than some thermobarometric estimates, which give peak pressures at the quartz-coesite boundary (Zhang *et al.*, 2005; Menold *et al.*, 2007, 2009).

In this paper, we report the first record of a coesite inclusion and inclusions of Ab + Qtz (mineral abbreviation after Kretz, 1983) assemblage in garnet from eclogites in the Yuka terrane at the western end of the North Qaidam UH*P*M belt. We show detailed petrography, present new constraints on the *P-T* evolution of the eclogites, and discuss the tectonic implications.

0935-1221/09/0021-1989 $ 6.30
DOI: 10.1127/0935-1221/2009/0021-1989

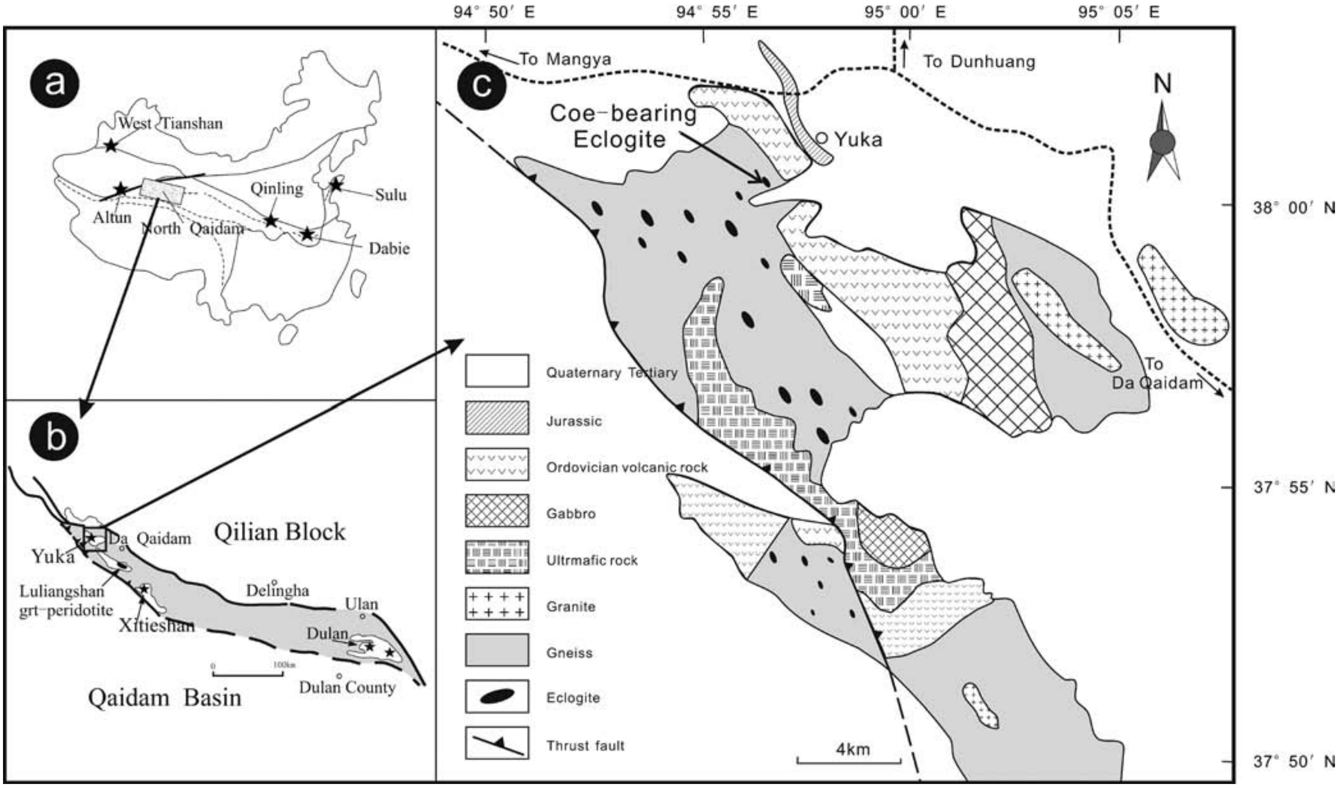

Fig. 1. Geological sketch map showing the distribution of recognized UH*P* metamorphic rocks along the North Qaidam UH*P* metamorphic belt, China (a), and distribution of eclogites in the Yuka area (b) (modified after Zhang *et al.* 2005).

2. Geological setting

The Paleozoic North Qaidam UH*P*M belt is bounded to the southwest by the Qaidam Block, and to the northeast by the Qilian Block (Fig. 1a) at the northern margin of the Tibetan Plateau (Fig. 1a). The Qaidam Block is a Cenozoic intra-continental basin developed on the Precambrian basement (*e.g.*, Yin *et al.*, 2002). The Qilian Block comprises mainly Paleozoic sedimentary rocks underlain by an imbricate thrust belt of Precambrian basement, which consists of granitic gneiss, pelitic gneiss, schist and marble (*e.g.*, Song *et al.*, 2009). The Altun H*P*/UH*P* rocks to the northwest are believed to be the northwestward extension of the North Qaidam UH*P*M belt (Fig. 1a), offset by the Cenozoic left-lateral Altyn Tagh fault zone (Liu *et al.*, 1999; Yin Harrison, 2000; Zhang *et al.*, 2001, 2005; Mattinson *et al.*, 2007). Along the North Qaidam UH*P*M belt, eclogites are found as blocks and interlayers within para- and orthogneisses in several localities (*e.g.*, Yuka, Xitieshan, and Dulan) extending, from northwest to southeast, for about 400 km (Fig. 1a). In addition, a garnet-bearing peridotite is exposed at the southern end of Lüliangshan area (Fig. 1a) (Yang & Deng, 1994; Song *et al.*, 2004, 2005a, b; Yang & Powell, 2008).

Our study area, the Yuka terrane, is situated at the northwestern end of the North Qaidam UH*P*M belt (Fig. 1a, b). Eclogites mainly occur as lentoid blocks (one to tens of metres in size; Figs 1b, 2a) and interlayers (Fig. 2c) within granitic gneisses and mica schists (Chen *et al.*, 2005; Zhang *et al.*, 2005; Menold *et al.*, 2007, 2009). Most eclogites are well preserved (Fig. 2b), but some are rimmed by retrograde/foliated amphibolite (Fig. 2d). The retrograde rims are isofacial with the gneisses, indicating that the eclogites and the host gneisses experienced the same retrogression and deformation. The granitic gneisses mainly consist of Qtz + Pl + Kfs + Czo + Ms, and the micaschists Qtz + Phn + Grt + Ky + Pl + Rt (Zhang *et al.*, 2004; Menold *et al.*, 2009).

Two types of eclogite, coarse- and fine-grained, are recognized. There are no obvious differences in the field occurrences of these eclogite types.

3. Analytical methods

Twenty-eight samples of both eclogites and country rocks were collected from the Yuka terrane. Five coarse-grained eclogite samples (fresh 4Y06, 07, 08 from one block; retrogressed 4Y16, 17 from another block) and one fine-grained eclogite sample (fresh 4Y18) have been studied in detail. Chemical compositions and element distribution mapping of minerals from the eclogites were analyzed using a JEOL JXA 6400 electron microprobe at the Electron Microscope Unit (EMU) of the Australian National University. Analytical conditions are accelerating voltage of 15 keV, 1 nA beam current, and 30 s counting time at

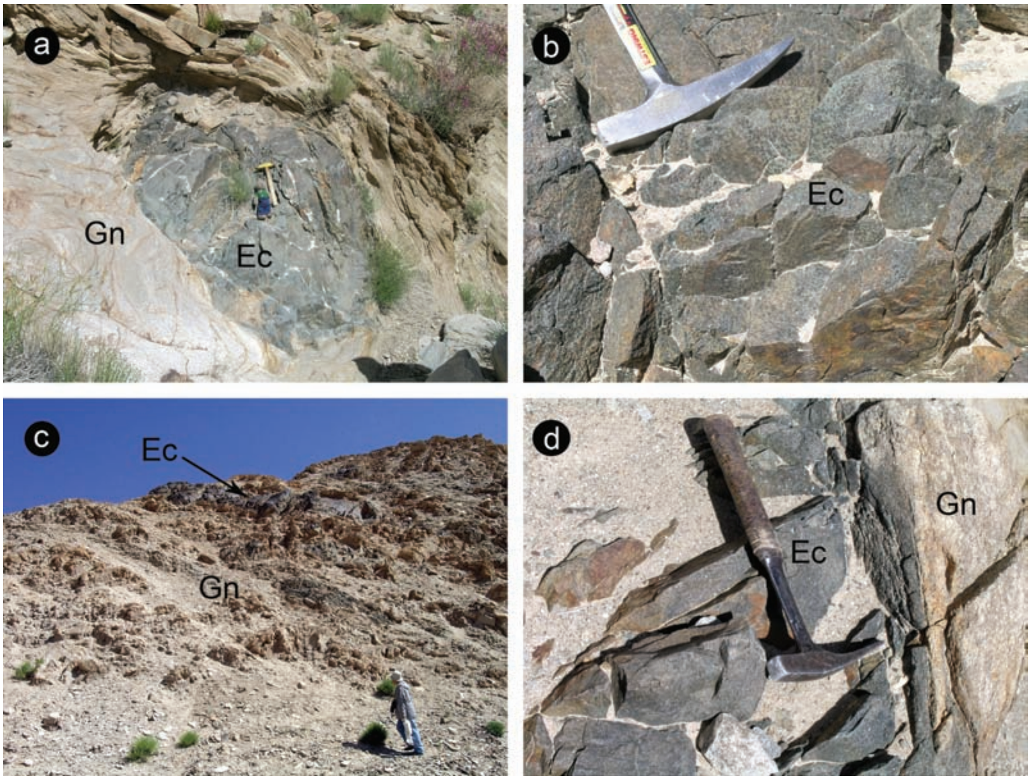

Fig. 2. Field views showing the occurrences of eclogites and associated country gneisses in the Yuka terrane, North Qaidam UH*P* metamorphic belt, China. (a) Lentoid eclogite block within the gneisses. (b) Fresh eclogite within the interiors of the lentoid blocks. (c) Eclogite as interlayers within the country gneisses. (d) The contact between eclogite and gneiss.

peak. Natural mineral standards and the ZAF matrix correction routine were used.

From the coarse-grained eclogite sample 4Y07, we found coesite and Ab + Qtz inclusions. Laser-Raman micro-spectroscopy (Renishaw RM-1000) at Peking University was used to confirm the coesite inclusion identified in a thin-section, with a 514.5 nm line Ar^{+} laser at 20–50 mW, 20–100 s measurement time, and a spectrum resolution of $\pm$ 1 cm^{-1}.

4. Petrography

Coarse-grained (~2 mm in size) eclogites are abundant, and record a complete metamorphic history of prograde, peak and retrograde conditions. Fine-grained (~0.5 mm in size) eclogites are less abundant; they are all fresh, well preserved, and have no retrogression. Hence, we used coarse-grained eclogites to constrain the metamorphic evolution and fine-grained eclogites to obtain additional constraints on prograde and peak metamorphic conditions.

4.1. Coarse-grained eclogites

Fresh coarse-grained eclogites consist of Grt (30–40 vol%), Omp (30–40 vol%), Phn (5–10 vol%), Qtz (~ 5 vol%) and Rt (<5 vol%) (Fig. 3a). Garnets are generally coarse porphyroblasts (1–2 mm, and >3 mm for the largest grain), surrounded by omphacite, phengite and quartz. Large garnet grains show obvious core-mantle structures (Fig. 3b, e). Epidote, amphibole, plagioclase and quartz are preserved as tiny inclusions in the garnet core, and a few phengite, omphacite and rutile crystals are preserved in the garnet mantle portion (Fig. 3b). The garnet mantle is generally surrounded by an inclusion-poor rim. The garnets are commonly rimmed by kelyphite of intergrown green amphibole and plagioclase as a result of decompression-induced decomposition reactions.

Clinopyroxene occurs in three textural types: inclusions in the garnet mantle (Cpx_1, Fig. 3b), coarse-grained crystals in the matrix (Cpx_2, Fig. 3a, b), and minor grains in the Cpx_3 + Pl symplectite ‘‘aggregates’’ after matrix omphacite.

Four types of amphibole have been distinguished in the eclogites: (1) Amp_1 occurs as inclusion in the garnet core (Fig. 3b); (2) Amp_2 symplectite coexisting with plagioclase after omphacite; (3) Amp_3 as corona amphibole around garnet rims; and (4) Amp_4 as product of retrogressed matrix omphacite (with some omphacite relics).

Phengite occurs both as inclusions (Phn_1) in the garnet mantle (Fig. 3b) and in the matrix (Phn_2) coexisting with garnet and omphacite (Fig. 3a).

4.2. Fine-grained eclogites

Fine-gained eclogites consist of Grt (40–50 vol%), Omp (40–45 vol%), Phn (<5 vol%), Ep (<5 vol%), Qtz (< 5

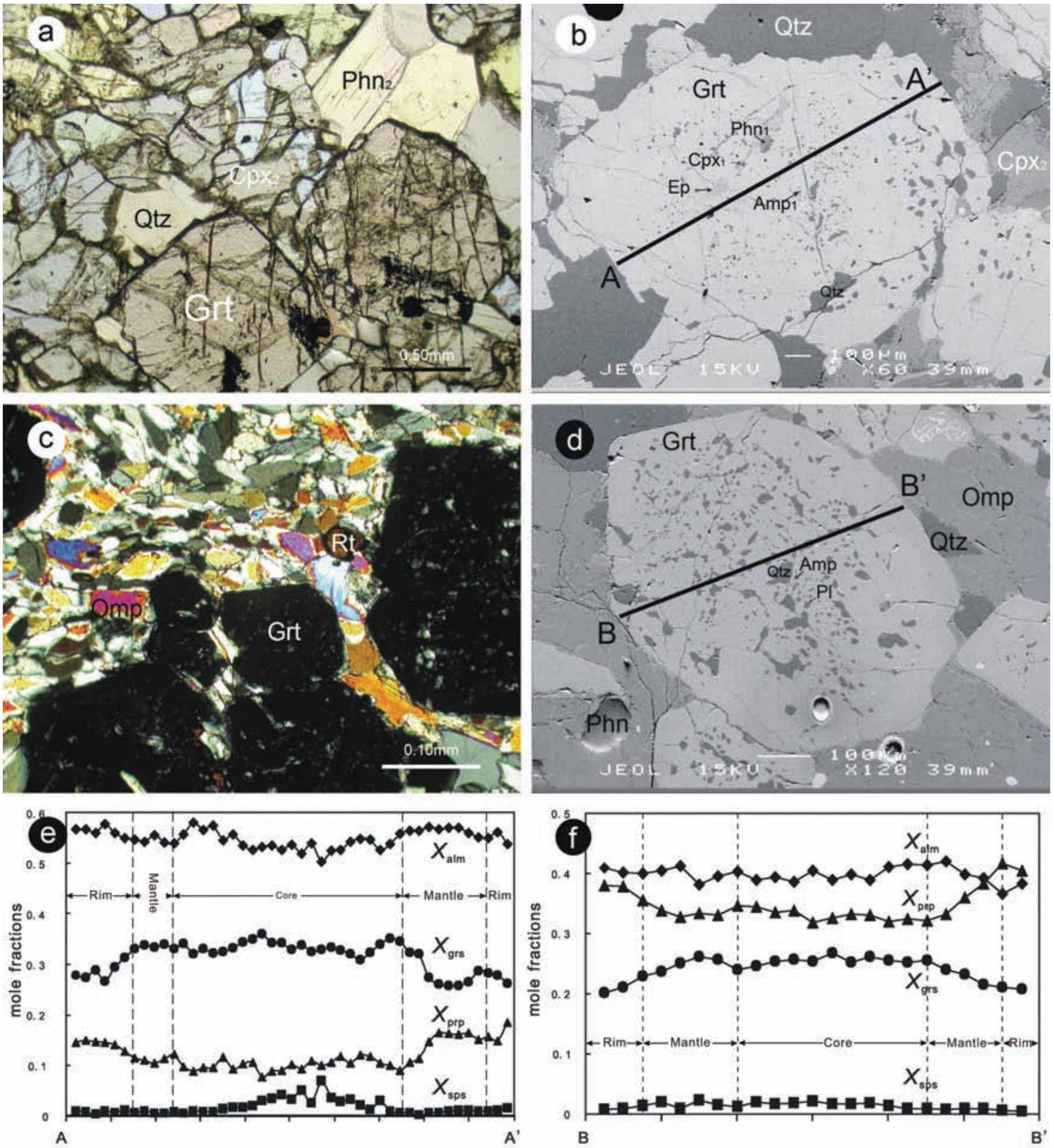

Fig. 3. Photomicrographs illustrating typical textures in both types of eclogites from the Yuka terrane, North Qaidam UH*P*M belt, China. (a) Garnet is surrounded by omphacite, phengite and quartz in the coarse-grained eclogite (4Y07, under plane-polarised light). (b) Mineral inclusions in the core and mantle of garnet in the coarse-grained eclogites (4Y06, BSE image). (c) Idiomorphic garnet with small omphacite, phengite and rutile in the fine-grained eclogites (4Y18, under crossed nicols). (d) Idiomorphic garnet contains abundant quartz inclusions with minor amphibole and feldspar in the fine-grained eclogites (4Y18, BSE image). (e) Compositional zoning profile of the garnet in b. (f) Compositional zoning profile of the garnet in d.

vol%) and Rt (~ 1 vol%) (Fig. 3c). All the minerals are smaller in grain size (generally ~0.5 mm) than in the coarse-grained eclogites. Most garnet crystals are idiomorphic (Fig. 3c, d). Minor epidote, amphibole and plagioclase inclusions are present in these garnets (Fig. 3d).

On the basis of mineral inclusion assemblages of the two types of eclogites and alteration mineral assemblages in the coarse-grained eclogites, three main metamorphic stages can be defined: pre-peak, peak and retrograde stages. The pre-peak and peak stages are recorded by both types of the eclogites, whereas the retrograde stage is only constrained by the retrogressed coarse-grained eclogites. In the coarse-grained eclogites, the inclusion assemblage of Amp + Ep + Pl + Qtz in the garnet core and the inclusion assemblage of Cpx + Phn in the garnet mantle record prograde pre-peak stage. The assemblage of Grt + Omp + Phn + Qtz/Coesite + Rt represents the peak metamorphic conditions. During retrogression, matrix omphacite altered first at the rims, followed later pervasively to a Cpx + Pl symplectite, which is replaced still later by Amp + Pl assemblage. Also, some garnets are rimmed by kelyphitic amphibole and plagioclase during decompression.

In the fine-grained eclogites, the inclusion assemblage of Amp + Pl + Qtz in the garnet core represents the prograde stage. The peak assemblage is Grt + Omp + Phn + Ep + Qtz + Rt.

5. Mineral chemistry

5.1. Coesite inclusion

Out of the 28 thin sections examined, we found only one coesite inclusion in sample 4Y07. The coesite inclusion occurs in a garnet rim portion (Fig. 4). The garnet grain is about 0.8 mm in the longer dimension (Fig. 4a). The coesite and its surrounding aggregates of palisade quartz are surrounded by weak radial fractures in the host garnet (Fig. 4c, d). The quartz inclusion was shaped like a trapezium with a long tail under BSE image (Fig. 4a, c), and the more refractive coesite relic (~10 µm) was preserved at the centre of the trapezium-shape part of the quartz (~30 µm) (Fig. 4d). A Raman microspectroscopic analysis of the central relic shows the characteristic coesite band at 522 cm^{-1} with subsidiary bands at 431, 355, and 273 cm^{-1} (Fig. 5a). The 464 cm^{-1} band for retrograde quartz is also visible (Fig. 5a). The surrounding quartz shows a strong band at 466 cm^{-1} (Fig. 5b).

5.2. Ab + Qtz inclusion assemblage

In several samples, we found inclusions of an Ab + Qtz association in garnet (Fig. 6). In the same thin section 4Y07, pure quartz (confirmed by Raman analysis) is surrounded by almost pure albite (An_3) within garnet, and develops very strong radial fractures in the host garnet (Fig. 6a, b). In another Ab + Qtz inclusion in thin section 4Y06, there are no obvious cracks in the surrounding garnet (Fig. 6c, d). These entrapped mineral inclusion assemblages are not zoned. No significant halos or garnet zoning adjacent to the inclusion assemblage have been found at the scale of the EMP analysis, which indicates little or no compositional exchange between the inclusion assemblages and the host garnet. The well-developed cracks around the inclusion assemblage in sample 4Y07 resemble the features typically caused by volume expansion in transforming from coesite to quartz (Chopin, 1984; Smith, 1984). Hence, we deduce that the compound inclusion may have experienced a dramatic volume expansion. One possibility may be expressed by the reaction of the form coesite + jadeite → quartz + albite upon decompression. There will be an associated volume expansion of up to 24 %. This requires the coexistence of omphacite (diopside + jadeite solid solutions) and jadeite, which is possible in disequilibrium situation.

5.3. Garnet

End-member compositions of garnet were calculated using Fe^{2+}/Fe^{3+} ratios estimated from charge-balance and stoichiometry (Droop, 1987). Compared to the fine-grained eclogite, the coarse-grained eclogite has garnet porphyroblasts with higher $X_{alm}[=Fe/(Fe^{2+} + Mn + Mg + Ca) = 0.46-0.60]$, and contain various amounts of

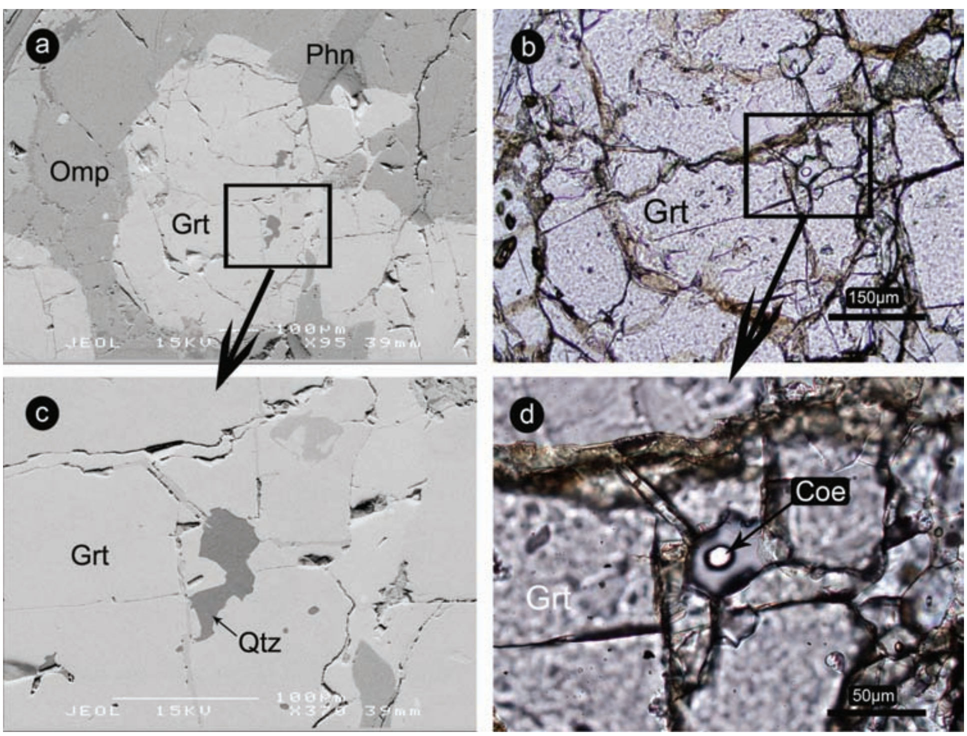

Fig. 4. BSE images (a) and (c) showing coesite inclusions in garnet, and the corresponding microphotographs (b) and (d) (4Y07, coarse-grained eclogite).

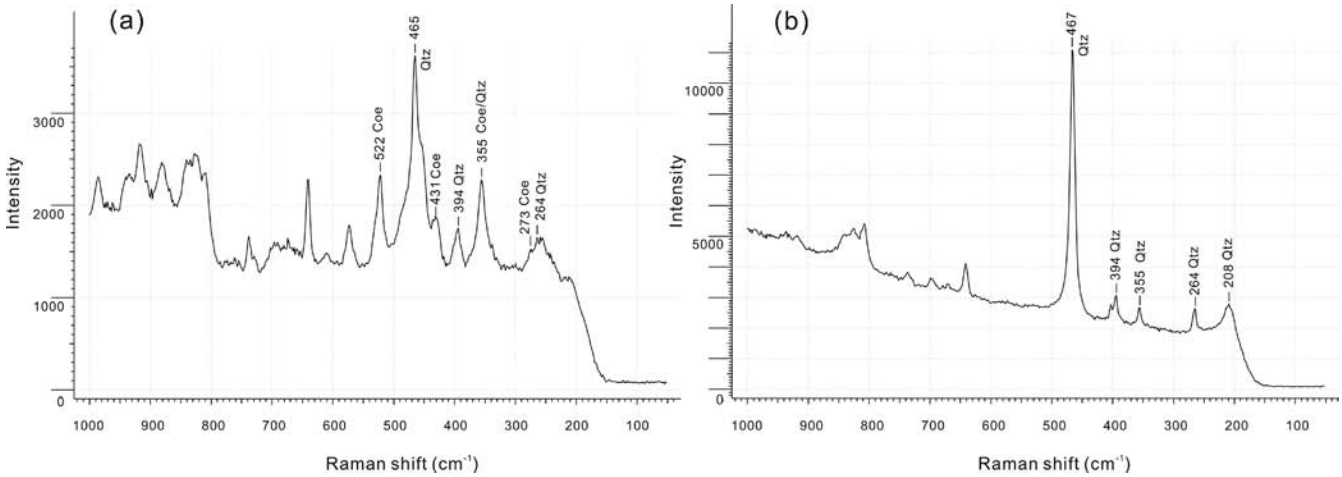

Fig. 5. Raman spectra in the range of 100–1000 cm^{-1} for the coesite inclusion in garnet (unlabeled bands belong to garnet or section resin mount). (a) Raman spectrum of coesite relic in the Fig. 4. (b) Raman spectrum of the surrounding retrogressed quartz in the Fig. 4.

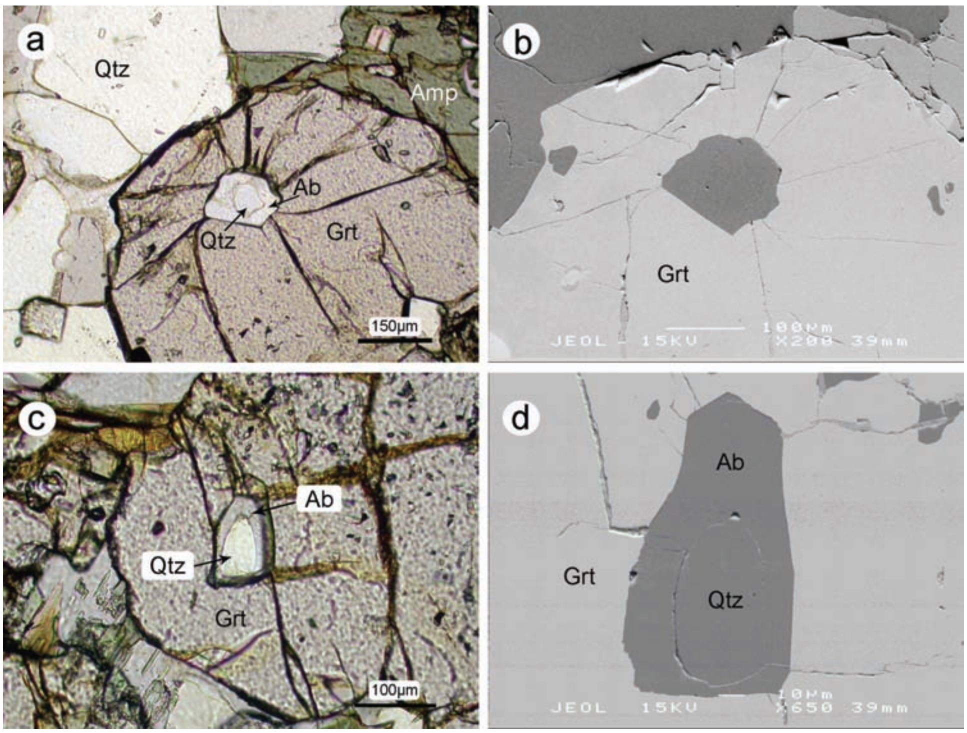

Fig. 6. Microphotographs (a) and (c) showing the Ab + Qtz inclusion assemblage in garnet and corresponding BSE images (b) and (d).

X_{pyp}(0.06–0.29), X_{grs}(0.23–0.37), and minor X_{sps}($<$0.07) (Table 1, Fig. 7a). Most garnet grains from the fresh samples show conspicuous compositional zoning (Fig. 3b, e). Similar to the inclusion assemblage domains in the garnet, the compositional zoning profile can be divided into core, mantle and rim parts. From core to rim, the X_{grs} and X_{sps} decrease with associated X_{pyp} increase (Fig. 3e).

Compared to the coarse-grained eclogites, garnet in the fine-grained eclogites has higher MgO and lower FeO as reflected in the mole fractions of end-members: X_{alm}, 0.38–0.41; X_{pyp}, 0.30–0.41; X_{grs}, 0.20–0.26; and minor X_{sps}, 0.01–0.03 (Table 1). Some zoning is also visible in the garnet of the fine-grained eclogites (Fig. 3d, f).

5.4. Clinopyroxene

Clinopyroxene contains up to 43 % jadeite. The Fe^{3+} content in clinopyroxene is assumed to be $Fe^{3+} = Na - (Al + Cr)$. For the coarse-grained eclogites, most of the clinopyroxene inclusions (Cpx_1) and the matrix omphacite (Cpx_2) have similar compositions regardless of the mode of occurrence (Table 2), suggesting that most of the inclusions and matrix clinopyroxenes were formed at the same

Table 1. Representative analyses of garnet in eclogites from the Yuka terrane, North Qaidam UH*P* metamorphic belt, China.

	Coarse-grained eclogite												Fine-grained eclogite	
	4Y06		4Y07		4Y06		4Y07		4Y08		4Y16		4Y18	
Sample	Core	Rim	Core	Rim							Core	Rim	Rim	Core
SiO_2	37.73	37.96	38.23	38.26	37.92	37.44	38.72	37.78	38.37	38.96	37.69	37.69	40.18	38.80
TiO_2	0.04	0.09	0.11	0.08	0.00	0.16	0.00	0.04	0.01	0.07	0.00	0.08	0.01	0.12
$A1_2O_3$	20.92	20.95	21.11	21.46	21.20	20.94	21.63	21.50	21.43	21.79	21.36	20.55	22.56	21.80
Cr_2O_3	0.10	0.12	0.00	0.07	0.00	0.01	0.00	0.03	0.00	0.06	0.05	0.06	0.04	0.04
FeO	26.36	25.86	26.06	26.95	26.08	27.98	24.47	24.49	25.49	22.09	27.61	28.69	19.33	21.01
MnO	0.25	0.68	0.51	1.11	0.51	0.55	0.45	0.42	0.79	0.32	1.01	0.52	0.41	1.20
MgO	1.62	4.61	2.90	4.06	3.91	1.71	4.53	3.56	6.45	5.18	3.07	2.96	10.72	7.91
CaO	13.05	9.07	11.38	8.20	9.94	10.99	10.95	11.44	6.62	11.49	9.79	9.27	7.41	9.11
Na_2O	0.13	0.24	0.21	0.15	0.18	0.24	0.12	0.28	0.19	0.23	0.11	0.17	0.12	0.14
K_2O	0.00	0.02	0.01	0.01	0.00	0.00	0.03	0.00	0.00	0.01	0.06	0.02	0.00	0.01
Total	100.20	99.60	100.52	100.35	99.74	100.02	100.90	99.54	99.35	100.20	100.75	100.01	100.78	100.14
Normalized to 8 cations and 12 oxygen														
Si	2.98	2.98	2.99	2.99	2.98	2.97	2.99	2.96	2.99	3.00	2.95	2.98	2.99	2.96
Ti	0.00	0.01	0.01	0.01	0.00	0.01	0.00	0.00	0.00	0.00	0.00	0.01	0.00	0.01
Al	1.94	1.93	1.94	1.98	1.96	1.96	1.97	1.98	1.97	1.98	1.97	1.92	1.98	1.96
Cr	0.01	0.01	0.00	0.00	0.00	0.00	0.00	0.00	0.00	0.00	0.00	0.00	0.00	0.00
Fe^{3+}	0.10	0.13	0.09	0.04	0.11	0.12	0.08	0.13	0.08	0.05	0.13	0.13	0.05	0.13
Fe^{2+}	1.64	1.57	1.61	1.72	1.60	1.74	1.50	1.48	1.58	1.37	1.68	1.77	1.16	1.21
Mn	0.02	0.05	0.03	0.07	0.03	0.04	0.03	0.03	0.05	0.02	0.07	0.04	0.03	0.08
Mg	0.19	0.54	0.34	0.47	0.46	0.20	0.52	0.42	0.75	0.59	0.36	0.35	1.19	0.90
Ca	1.10	0.76	0.95	0.69	0.84	0.93	0.91	0.96	0.55	0.95	0.82	0.79	0.59	0.74
Na	0.02	0.04	0.03	0.02	0.03	0.04	0.02	0.04	0.03	0.03	0.02	0.03	0.02	0.02
K	0.00	0.00	0.00	0.00	0.00	0.00	0.00	0.00	0.00	0.00	0.00	0.00	0.00	0.00
Sum	8.00	8.00	8.00	8.00	8.00	8.00	8.00	8.00	8.00	8.00	8.00	8.00	8.00	8.00
X_{alm}	0.55	0.54	0.55	0.58	0.55	0.60	0.51	0.51	0.54	0.47	0.60	0.57	0.39	0.41
X_{sps}	0.01	0.02	0.01	0.03	0.01	0.01	0.01	0.01	0.02	0.01	0.01	0.02	0.01	0.03
X_{pyp}	0.06	0.18	0.12	0.16	0.16	0.07	0.18	0.14	0.26	0.20	0.12	0.12	0.40	0.31
X_{grs}	0.37	0.26	0.32	0.23	0.29	0.32	0.31	0.33	0.19	0.32	0.27	0.28	0.20	0.25

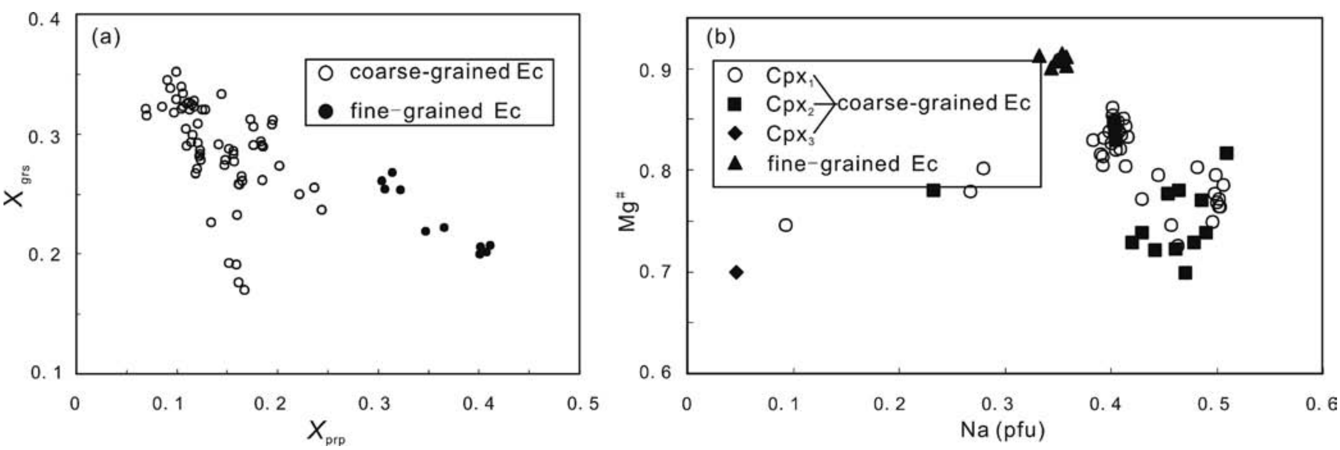

Fig. 7. Compositional range of garnets (a) and clinopyroxenes (b) in both coarse- and fine-grained eclogites.

stage (near peak). Some Cpx_1 have lower jadeite content (Table 2, Jd = 19.64 %), indicating that they were probably formed before the peak stage. The later modification (retrogression) of Cpx_2 composition is ubiquitous with Si and Na decreasing from core to rim (Jd < 10% for the rim of altered matrix omphacite; Table 2). Further decompression breakdown of the matrix omphacite produces symplectites of Na-poor Cpx_3 (Jd 2–5 %, Table 2) + Pl, some of which were completely replaced by later Amp + Pl. Clinopyroxenes in fine-grained eclogites are all fresh,

Table 2. Representative analyses of clinopyroxene in eclogites from the Yuka terrane, North Qaidam UH*P* metamorphic belt, China

	Coarse-grained eclogite									Fine-grained eclogite		
	4Y06		4Y07	4Y17	4Y07			4Y06		4Y18		
	Cpx1				Cpx2				Cpx3	matrix		
Sample					Core	Rim	Core	Rim				
SiO_2	55.70	53.03	56.07	54.97	56.32	55.05	56.11	53.71	54.32	55.63	55.84	56.45
TiO_2	0.21	0.25	0.23	0.13	0.00	0.10	0.00	0.13	0.11	0.02	0.08	0.06
Al_2O_3	10.50	6.17	9.87	9.01	9.57	8.36	9.73	2.61	6.13	8.55	8.99	9.01
Cr_2O_3	0.11	0.13	0.03	4.19	0.00	0.00	0.00	0.17	0.09	2.00	2.02	2.16
FeO	5.86	7.38	4.06	4.87	2.53	6.02	3.83	7.39	9.45	0.25	0.15	0.23
MnO	0.00	0.00	0.03	0.00	0.04	0.12	0.01	0.10	0.00	0.02	0.05	0.01
MgO	7.75	10.16	9.69	7.54	10.61	9.23	9.62	12.14	12.36	11.59	11.03	11.22
CaO	12.15	19.13	15.01	12.98	15.40	16.29	14.46	22.41	17.18	16.71	16.02	16.28
Na_2O	7.38	3.26	5.90	6.66	5.51	5.05	6.03	1.30	0.64	4.80	5.01	5.24
K_2O	0.00	0.01	0.02	0.01	0.00	0.02	0.00	0.03	0.65	0.00	0.01	0.06
Total	99.66	99.52	100.91	100.36	99.98	100.24	99.79	99.99	100.93	99.57	99.20	100.72
Cations per 6 oxygen atoms												
Si	1.99	1.95	1.98	1.98	2.00	1.98	2.00	1.99	2.00	1.99	2.00	1.99
Ti	0.01	0.01	0.01	0.00	0.00	0.00	0.00	0.00	0.00	0.00	0.00	0.00
Al	0.44	0.27	0.41	0.38	0.40	0.36	0.41	0.11	0.27	0.36	0.38	0.37
Cr	0.00	0.00	0.00	0.00	0.00	0.00	0.00	0.01	0.00	0.01	0.00	0.01
Fe^{3+}	0.07	0.05	0.00	0.08	0.00	0.00	0.00	0.00	0.00	0.00	0.00	0.00
Fe^{2+}	0.11	0.18	0.12	0.18	0.08	0.18	0.11	0.23	0.29	0.06	0.06	0.06
Mn	0.00	0.00	0.00	0.00	0.00	0.00	0.00	0.00	0.00	0.00	0.00	0.00
Mg	0.41	0.56	0.51	0.41	0.56	0.50	0.51	0.67	0.68	0.62	0.59	0.59
Ca	0.46	0.75	0.57	0.50	0.59	0.63	0.55	0.89	0.68	0.64	0.62	0.62
Na	0.51	0.23	0.40	0.47	0.38	0.35	0.42	0.09	0.05	0.33	0.35	0.36
K	0.00	0.00	0.00	0.00	0.00	0.00	0.00	0.00	0.03	0.00	0.00	0.00
Sum	4.00	4.00	4.00	4.00	4.00	4.00	4.00	4.00	4.00	4.00	4.00	4.00
Jd	43.0	19.6	38.6	46.9	38.3	32.6	40.6	9.4	5.3	33.5	35.5	36.1
$Mg^{\#}$	0.82	0.75	0.84	0.78	0.88	0.77	0.83	0.75	0.70	0.91	0.91	0.90

with slightly lower jadeite content (Jd: 33–37%) and higher $Mg^{\#}$ (0.90–0.91) (Table 2) than those of matrix omphacite in the coarse-grained eclogite.

5.5. Amphibole

According to the classification scheme of Leake *et al.* (1997; Fig. 8), all the amphiboles belong to the calcic group. For the coarse-grained eclogites, the amphibole inclusions in the garnet core are mainly edenite, but some are pargasite and ferrotschermakite (Table 3, Fig. 8). The corona amphibole around the garnet rims is ferropargasite. Those associated with the symplectitic Cpx + Pl (after omphacite) and the retrogressed amphibole are edenite (Table 3, Fig. 8).

The amphibole inclusions in garnet of the fine-grained eclogites are mainly actinolite, but some may be classified as magnesiohornblende (Table 3, Fig. 8).

5.6. Phengite

Most phengite inclusions (Si $= 3.38-3.46$) in mantle portions of the garnet in the coarse-grained eclogites and the matrix phengite (Si $= 3.42-3.46$) have similar compositions (Table 4). This implies that most phengite inclusions in the garnet mantle portion were formed during the peak metamorphic stage. Some lower-Si (Si $= 3.26$) phengite inclusions may have formed before the peak. Matrix phengite shows very small compositional variation from core to rim (Table 4). A few matrix phengites show lower Si content (Si $=$ 3.26–3.28) (Table 4) probably influenced by retrograde modification.

The phengite in the fine-grained eclogites is homogeneous in composition, as shown by microprobe analysis and BSE analysis. It has 3.41–3.52 Si per 11 oxygens formula unit (Table 4).

5.7. Feldspar

Feldspars in the coarse-grained eclogites occur (1) as rare oligoclase (An_{13-17}) and albite ($An < 5$) coexisting with quartz inclusions in the garnet core of coarse-grained eclogites; (2) as a component (with An_{3-5}) of symplectite after matrix omphacite; (3) as a constituent of kelyphite rims around garnet associated with amphibole (An_{4-7}); and (4) in the highly retrogressed eclogite (An_{11-18}) (Table 4).

Rare albite (An_7) inclusions were also found in the garnet core of the fine-grained eclogites (Table 4).

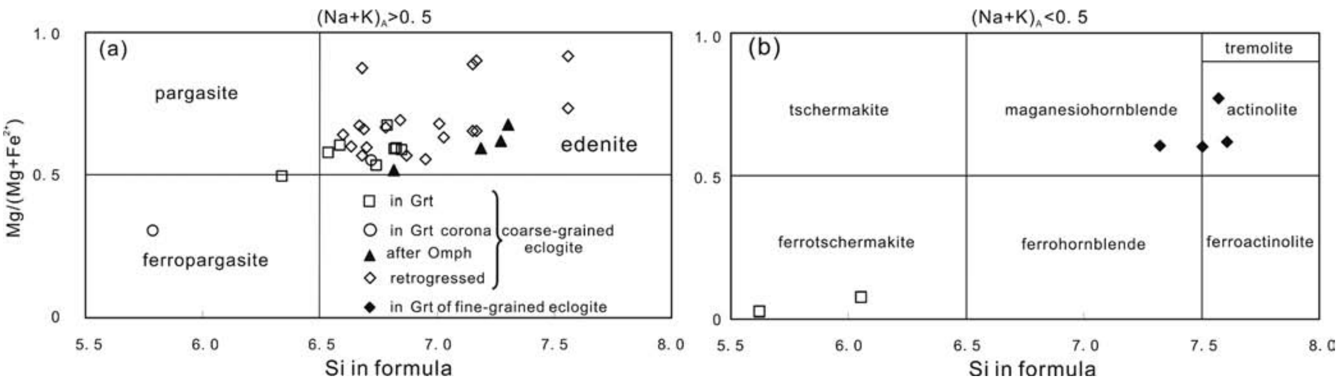

Fig. 8. Classification diagrams for amphiboles in both coarse- and fine-grained eclogites following Leake *et al.* (1997).

Table 3. Representative analyses of amphibole in eclogites from the Yuka terrane, North Qaidam UH*P* metamorphic belt, China

	Coarse-grained eclogite											Fine-grained eclogite	
	$Amph_1$ incl. in Grt			ph_2 sym. after O_1		mph_3 sym. after G		Retrogressed $Amph_4$				Inclusion in Grt	
	4Y07	4Y17		4Y16	4Y07	4Y06	4Y17	4Y06		4Y17		4Y18	
Sample		Core	Rim					Core	Rim				
SiO_2	44.57	44.70	35.22	49.96	45.05	44.21	37.42	44.45	51.57	44.86	47.12	51.25	50.39
TiO_2	0.53	0.66	0.25	0.29	0.44	0.43	0.09	0.34	0.16	0.48	0.39	0.17	0.05
$A1_2O_3$	14.90	12.55	18.95	6.92	8.61	12.83	18.11	14.35	6.18	14.24	13.27	4.14	5.60
Cr_2O_3	0.00	0.12	0.00	0.02	0.00	0.04	0.08	0.17	0.03	0.00	10.73	0.03	0.07
FeO	14.85	16.66	24.59	12.09	19.54	15.33	22.40	15.48	11.94	13.80	0.02	16.52	16.32
MnO	0.14	0.13	0.68	0.10	0.06	0.14	0.17	0.00	0.00	0.02	0.01	0.06	0.22
MgO	9.46	9.23	3.69	14.21	9.76	10.00	4.64	9.59	14.78	10.18	12.70	12.78	12.65
CaO	9.34	7.65	10.73	12.04	11.24	10.41	10.93	7.61	8.25	8.60	9.18	11.86	12.22
Na_2O	2.89	4.17	2.58	1.19	1.75	2.90	2.59	4.56	3.57	3.85	3.59	0.86	1.03
K_2O	0.51	0.74	0.32	0.12	0.08	0.83	0.17	0.86	0.44	0.59	0.55	0.18	0.09
Total	97.19	96.61	97.01	96.94	96.53	97.12	96.60	97.41	96.92	96.62	97.56	97.85	98.64
Si	6.74	6.66	5.46	7.30	6.81	6.72	5.78	6.68	7.56	6.87	7.01	7.51	7.32
Ti	0.06	0.07	0.03	0.03	0.05	0.05	0.01	0.04	0.02	0.06	0.04	0.02	0.01
Al	2.65	2.21	3.47	1.19	1.54	2.30	3.30	2.54	1.07	2.57	2.33	0.71	0.96
Cr	0.00	0.01	0.00	0.00	0.00	0.01	0.01	0.02	0.00	0.00	0.00	0.00	0.01
Fe^{3+}	0.00	0.33	0.96	0.00	0.40	0.00	0.53	0.31	0.30	0.00	0.00	0.17	0.18
Fe^{2+}	1.88	1.74	2.23	1.48	2.07	1.95	2.36	1.64	1.17	1.77	1.34	1.86	1.81
Mn	0.02	0.02	0.09	0.01	0.01	0.02	0.02	0.00	0.00	0.00	0.00	0.01	0.03
Mg	2.13	2.05	0.85	3.10	2.20	2.27	1.07	2.15	3.23	2.32	2.82	2.79	2.74
Ca	1.51	1.22	1.78	1.89	1.82	1.70	1.81	1.23	1.30	1.41	1.46	1.86	1.90
Na	0.85	1.21	0.78	0.34	0.51	0.86	0.78	1.33	1.02	1.14	1.04	0.24	0.29
K	0.10	0.14	0.06	0.02	0.02	0.16	0.03	0.17	0.08	0.12	0.10	0.03	0.02
Sum	15.95	15.66	15.72	15.36	15.43	16.02	15.70	16.09	15.73	16.26	16.14	15.21	15.26

5.8. Epidote

The epidote inclusion preserved in the garnet core of the coarse-grained eclogites has 0.10−0.18 X_{ps} (Fe^{3+} / (Fe^{3+} + Al)) (Table 4), whereas the matrix epidote in the fine-grained eclogite has lower X_{ps} (∼0.05) (Table 4).

6. *P-T* determination

The preservation of earlier mineral assemblages as inclusions in peak metamorphic minerals and as retrograde overprints in the same rock enables us to deduce conditions at various stages of the metamorphic histories of the rock samples. We obtained the *P-T* paths from thermobarometric calculations using the established phase equilibria.

6.1. Pre-peak stage

Prograde growth history can be recorded by mineral assemblages preserved as inclusions in garnet. To use them with confidence, the inclusion minerals should retain the original composition and have avoided subsequent re-equilibration among them and with the host garnet. Detailed petrography and microprobe analysis indicate

Table 4. Representative analyses of phengite, feldspar and epidote in eclogites from the Yuka terrane, North Qaidam UH*P* metamorphic belt, China.

	Coarse-grained eclogite																Fine-grained eclogite			
	4Y06	4Y07	4Y16		4Y06	4Y07		4Y08		4Y07		4Y06	4Y17		4Y07		4Y18			
	Phn_1 incl. in Grt				Matrix Phn_2					Feldspar					Ep incl. in Grt		Matrix phengite		Matrix Ep	Ab incl. in Grt
Sample								Core	Rim	In Ab+Qtz	Incl. in Grt	Sym. after Omph	Sym. after Grt	Retrogressed						
SiO_2	48.25	50.60	50.51	51.37	48.72	48.03	50.88	50.74	50.80	68.36	64.56	67.29	65.59	64.50	38.54	38.26	52.34	51.41	38.41	66.96
TiO_2	0.62	0.54	0.89	0.66	0.89	0.71	0.59	0.62	0.54	0.01	0.04	0.04	0.06	0.89	0.35	0.19	0.32	0.39	1.11	0.08
Al_2O_3	29.71	26.36	26.65	24.91	28.73	29.83	26.15	26.21	26.53	20.27	21.82	19.63	18.75	18.52	29.89	26.46	24.81	25.84	30.65	20.70
Cr_2O_3	0.04	0.00	0.19	0.15	0.09	0.00	0.06	0.01	0.00	0.00	0.01	0.09	0.00	0.09	0.05	0.00	0.08	0.10	0.01	0.02
FeO	1.96	2.17	1.67	2.97	2.59	1.83	1.92	1.95	1.55	0.31	0.75	0.24	0.86	1.40	4.47	8.00	0.85	0.98	2.21	0.55
MnO	0.02	0.12	0.00	0.00	0.08	0.05	0.00	0.08	0.00	0.00	0.00	0.01	0.00	0.03	0.00	0.00	0.00	0.00	0.02	0.00
MgO	2.64	3.61	3.94	3.91	2.95	2.53	3.66	3.61	3.87	0.11	0.01	0.00	0.51	1.51	0.30	0.18	4.76	4.66	0.16	0.02
CaO	0.01	0.08	0.11	0.00	0.00	0.00	0.04	0.08	0.00	0.49	3.12	0.56	1.23	2.07	23.64	22.06	0.03	0.02	23.95	1.44
Na_2O	0.97	0.35	0.64	0.47	0.82	1.01	0.41	0.60	0.42	10.87	9.97	11.17	10.56	9.66	0.09	0.03	0.39	0.53	0.08	10.94
K_2O	9.76	9.77	10.27	10.45	9.92	9.53	10.05	9.32	10.41	0.02	0.05	0.01	0.00	0.02	0.03	0.00	10.05	10.50	0.05	0.05
Total	93.98	93.60	94.87	94.89	94.79	93.53	93.76	93.22	94.12	100.44	100.33	99.04	97.56	98.69	97.36	95.18	93.63	94.43	96.65	100.76
Si	3.26	3.42	3.38	3.46	3.28	3.26	3.44	3.42	3.46	2.97	2.84	2.97	2.95	2.89	2.97	3.04	3.52	3.44	2.97	2.92
Ti	0.03	0.03	0.05	0.03	0.05	0.04	0.03	0.03	0.03	0.00	0.00	0.00	0.00	0.03	0.02	0.01	0.02	0.02	0.07	0.00
Al	2.36	2.10	2.10	1.98	2.28	2.38	2.08	2.10	2.04	1.04	1.13	1.02	0.99	0.98	2.72	2.48	1.97	2.04	2.80	1.06
Cr	0.00	0.00	0.01	0.01	0.01	0.00	0.00	0.00	0.00	0.00	0.00	0.00	0.00	0.00	0.00	0.00	0.00	0.01	0.00	0.00
Fe^{3+}	0.00	0.00	0.00	0.00	0.00	0.00	0.00	0.00	0.00	0.01	0.03	0.01	0.03	0.05	0.29	0.53	0.00	0.00	0.14	0.02
Fe^{2+}	0.11	0.12	0.09	0.17	0.15	0.10	0.11	0.09	0.08	0.00	0.00	0.00	0.00	0.00	0.00	0.00	0.05	0.06	0.00	0.00
Mn	0.00	0.01	0.00	0.00	0.01	0.00	0.00	0.00	0.00	0.00	0.00	0.00	0.00	0.00	0.00	0.00	0.00	0.00	0.00	0.00
Mg	0.27	0.36	0.39	0.39	0.30	0.26	0.37	0.39	0.42	0.01	0.00	0.00	0.03	0.10	0.03	0.02	0.48	0.47	0.02	0.00
Ca	0.00	0.01	0.01	0.00	0.00	0.00	0.00	0.00	0.00	0.02	0.15	0.03	0.06	0.10	1.95	1.88	0.00	0.00	1.99	0.07
Na	0.13	0.05	0.08	0.06	0.11	0.13	0.05	0.06	0.05	0.92	0.85	0.96	0.92	0.84	0.01	0.01	0.05	0.07	0.01	0.92
K	0.84	0.84	0.88	0.90	0.85	0.83	0.87	0.89	0.88	0.00	0.00	0.00	0.00	0.00	0.00	0.00	0.86	0.90	0.01	0.00
Sum	7.01	6.94	6.99	7.00	7.01	7.00	6.95	6.97	6.95	4.97	5.00	4.99	5.00	4.99	8.01	7.95	6.94	7.00	8.00	5.00

that most inclusions have not re-equilibrated significantly with the garnet. Applications of the Grt-Amp thermometer (Graham & Powell, 1984) and Grt-Amp-Pl-Qtz barometer (Kohn & Spear, 1990) to mineral inclusions in the garnet core and the host garnet in both types of the eclogites yield equilibration conditions of $P = 0.8$–1.0 GPa, $T = 450-560$ °C for the coarse-grained eclogites and $P = 1.0$–1.2 GPa, $T = 450-510$ °C for the fine-grained eclogites (see ''A'' in Fig. 9). These results, in conjunction with the presence of an oligoclase feldspar in the garnet core, indicate that the garnet experienced epidote-amphibolite-facies conditions prior to the peak metamorphism.

The garnet mantle portion in the coarse-grained eclogites contains some low-Na Cpx_1 and low-Si phengite inclusions, likely formed before the peak stage. Applying the Grt-Omp-Phn thermobarometry of Ravna & Terry (2004) to this inclusion assemblage and host garnet, we found $P = 2.25$–2.65 GPa, $T = 550$–610 °C (see ''B'' in Fig. 9), which indicates eclogite-facies conditions, but below the coesite stability field.

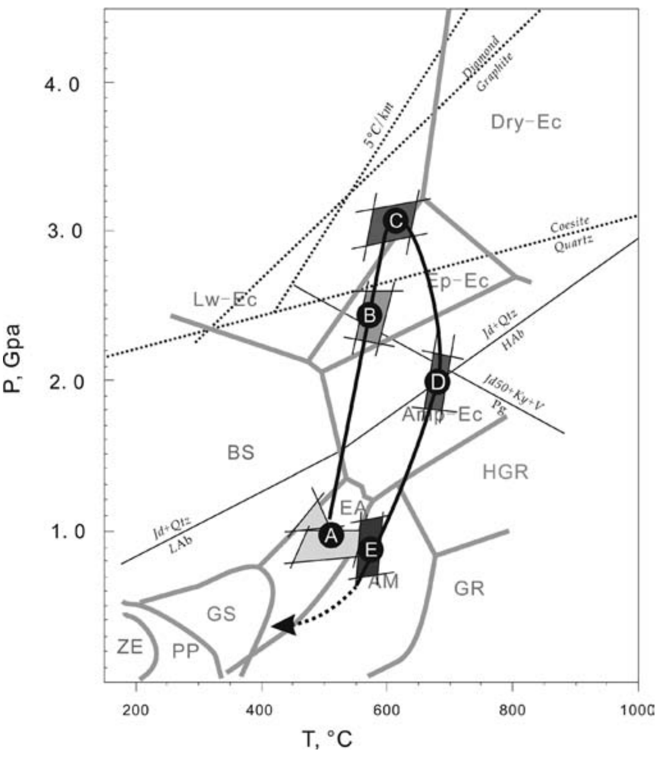

Fig. 9. P-T path for both coarse- and fine-grained eclogites from the Yuka terrane, North Qaidam UH*P*M belt, China (after Liou *et al.*, 1998). A, an earlier pre-peak stage constrained by the inclusion assemblage in the garnet core of both types of eclogites (the ranges are from five intersections of thermobarometry for each type eclogite); B, a later pre-peak stage constrained by the inclusion assemblage in the garnet mantle of coarse-grained eclogites (the range is from 6 intersections); C, a peak stage constrained by both types of eclogites (the range is from 6 intersections); D, an earlier retrograde stage constrained by retrogressed coarse-grained eclogites (the range is from 3 intersections); E, a later retrograde stage constrained by pervasively retrogressed coarse-grained eclogites (the range is from 5 intersections).

6.2. Peak stage

The occurrence of coesite inclusions in the coarse-grained eclogites demonstrates that the peak pressure must be in the coesite stability field. The peak mineral assemblage of the coarse-grained eclogites is Grt + Omp + Phn + Rt + Qtz/Coe; and for the fine-grained eclogites, Grt + Omp + Phn + Ep + Rt + Qtz/Coe(?). Using the Grt-Omp-Phn thermobarometer of Ravna & Terry (2004), the intersection of the Grt-Cpx-Phn and Grt-Cpx-SiO_2 thermobarometric curves in P-T space offers the best P-T estimates for peak conditions of the two types of eclogites. The highest X_{Mg} / $(X_{Mg} + X_{Fe})$ ratio in the garnet mantle has been selected to determine the peak P-T conditions (Carswell *et al.*, 1997) as given in Table 1. To minimize any retrogressive effect, we also chose omphacite with highest jadeite content in the freshest sample (Holland, 1980) and phengite with the highest Si content (Massonne & Schreyer, 1987). We thus obtained the peak conditions of $P = 3.01$GPa, $T = 652$ °C for the coarse-grained eclogites (4Y07), and $P = 2.9$–3.2 GPa, $T = 566$–613 °C for the fine-grained eclogites (4Y18), which are located in the coesite stability field (see ''C'' in Fig. 9).

6.3. Retrograde stage

The retrograde stage is constrained only by the alteration in the coarse-grained eclogites. Early stages of retrogression are recorded by the decreasing CaO at garnet rims, the decreasing jadeite content of the matrix omphacite and the lower Si in matrix phengite rims. Using the Grt-Omp-Phn thermobarometry of Ravna & Terry (2004), we obtained $P = 1.8$–2.5 GPa, $T = 670$–700 °C (see ''D'' in Fig. 9). Subsequently, the matrix omphacite broke down, acquired a rim of Cpx + Pl symplectite, and was finally replaced by Amp + Pl. The garnet developed an Amp + Pl corona. Using the Grt-Amp thermometer (Graham & Powell, 1984) and the Grt-Amp-Pl-Qtz barometer of Kohn & Spear (1990) on Grt-Amp-Pl retrograde mineral assemblages, we obtained equilibration temperatures of 550–590 °C and pressures of 0.7–1.1 GPa (see ''E'' in Fig. 9). Graham & Powell (1984) note that peak garnet and ''eclogitic amphiboles'' are generally in disequilibrium since they did not crystallise simultaneously, but their thermometer should nevertheless be useful for amphiboles that grew in equilibrium with resorbing garnet rims under amphibolite-facies conditions.

7. Discussion and conclusions

The North Qaidam UH*P*M belt extends about 400 km from southeast to northwest. The UH*P*M index mineral coesite was first found in zircons from pelitic gneisses in the Dulan terrane, the eastern end of this belt (Yang *et al.* 2001; Song *et al.*, 2003a). Coesite inclusions were recently reported in eclogite samples from the Shaliuhe cross section (Zhang *et al.*, 2009a) and south Dulan sub-belt (Zhang *et al.*, 2009b). For the western part of this belt, there are three major eclogite and garnet peridotite occurrences: Xitieshan, Yuka and Lüliangshan. Diamond inclusions in zircons and some exsolution textures had been reported from the Lüliangshan garnet peridotite, which suggested an origin at a depth of over 200 km (Song *et al.*, 2004, 2005a and b). For the two eclogite occurrences, only quartz exsolution was found from Xitieshan eclogite (Zhang *et al.*, 2005), and the significance of this texture remains controversial (Hermann *et al.*, 2005; Page *et al.*, 2005; Smith, 2005). Despite thermobarometry indicating UH*P*M conditions (or close to) for the Yuka eclogites (Chen *et al.*, 2005; Zhang *et al.*, 2005; Menold *et al.*, 2007), there has been no convincing evidence for UH*P* metamorphism. The present record of coesite inclusions in the Yuka eclogites provides the first direct evidence for UHPM for the western part of the North Qaidam UH*P*M belt.

A K-feldspar + quartz inclusion assemblage has been reported from eclogites in several UH*P*M terranes (Yang & Smith, 1989; Schmädicke, 1991; Yang *et al.*, 1998; Song *et al.*, 2003a; Zhang *et al.*, 2009c). Furthermore, the new mineral kokchetavite, a hexagonal high-pressure polymorph of K-feldspar, has been found from the Kokchetav UH*P*M terrane (Hwang *et al.*, 2004). This phase is metastable, and may be a decompression product of the stable high-pressure K-bearing assemblages such as wadeite-type $K_2Si_4O_9$ + kyanite + coesite at 6–9 GPa or hollandite-type $KAlSi_3O_8$ above 9 GPa (Ferroir *et al.*, 2006). The Ab + Qtz inclusions with strong evidence for volume expansion in our rocks offer new perspectives on UH*P*M and metamorphic histories. We consider two possible histories. One is the transformation from the relatively conventional dense phase jadeite plus the ultrahigh pressure SiO_2 phase coesite. Another is much less likely that these inclusions could have transformed from a very dense phase of $NaAlSi_3O_8$. This composition is stable in the hollandite structure in a limited pressure range of ~20–23 GPa at ~1000 °C (Liu, 1978) or higher temperatures (Yagi *et al.*, 1994). The Na-rich inclusions could also be produced by breakdown of the pre-peak amphibolite assemblage amphibole + plagioclase. Suppose the amphibole has some sodium on the A-site (*e.g.* pargasite), high-*P* and high-*T* breakdown reactions can be written that form jadeite:

(1) Prg +2 An + 2 Qtz → 7/3 Grt + Jd + H_2O
(2) Prg + 2 An + 2 Ab → 7/3 Grt + 3 Jd + H_2O
(3) Ab → Jd + Qtz

For reactions (1) and (2), Ca, Mg of amphibole and feldspar could diffuse into the host garnet, while Na and some Al and Si will form jadeite in the inclusion. Note that this accounts for the existence of jadeite as a second clinopyroxene phase included in the garnet, but out of equilibrium with the matrix omphacite. The water produced will escape before the peak metamorphic stage. The amphibole breakdown reactions are implied to have negative slope in *P-T* space, but this is consistent with known high-pressure stability of amphiboles (Evans, 2007).

In any case, radial fractures in garnet can be readily explained by volume expansion of the inclusion. The coesite → quartz transformation and the reaction coesite + jadeite → albite are both accompanied by volume increases that are large enough to fracture garnet easily: 13 % and 24 % respectively.

The *P-T* path in Fig. 9 illustrates the metamorphic evolution history of these two types of eclogites. The inclusion assemblage Amp + Ep + Pl + Qtz in the garnet core and the garnet zoning of the two types eclogites record prograde history and indicates that the garnet began to grow in the epidote-amphibole facies. The prograde path indicates a near isothermal compression process during subduction. The coesite inclusion (Fig. 4) (and the possible Jd + Coe precursor for the Ab + Qtz inclusion assemblage; Fig. 5) demonstrates that the coarse-grained eclogites experienced UH*P* metamorphism. This is further supported by the Grt-Omp-Phn thermobarometry at $P = 2.9$ GPa and $T = 652$ °C, which plots in the coesite stability field. The peak condition obtained using the thermobarometry for the fine-grained eclogites also indicates UH*P* metamorphism. The retrogression path for the coarse-grained eclogites is also a near isothermal decompression process, with only a slight temperature increase. Subsequently, the eclogites cooled and decompressed through the amphibolite-facies during exhumation. Compared with a few *P-T* paths of previous studies (Chen *et al.*, 2005; Zhang *et al.*, 2005; Menold *et al.*, 2007), our *P-T* path lends support to the result of Chen *et al.* (2005). The prograde conditions of Zhang *et al.* (2005) give slightly higher temperature, which may be an artefact of later re-equilibration of inclusions. And the peak pressure estimates by Zhang *et al.* (2005) and Menold *et al.* (2007) are near the coesite stability field but lower than ours.

The calculated geothermal gradient during subduction for the coarse-grained eclogites is about 6.5 °C km^{-1}, a similar value of 5.4–6.4 °C km^{-1} was obtained for the fine-grained eclogites. This is consistent with previous studies that have suggested that a low geothermal gradient (~7 °C km^{-1}) is conducive to preservation of coesite inclusions (Liou *et al.*, 2004). This means that the subducted lithosphere should be either old, cold, oceanic crust-capped lithosphere ± pelagic sediments or ancient continental crust (Liou *et al.*, 2004). For retrogression, Zhang *et al.* (2005) proposed an average cooling rate of 13–19 °C/My, and fast exhumation rates of 2–5 km/My. The preservation of garnet zoning and decompression texture of omphacite in our eclogite samples favour fast exhumation. Although both continental and oceanic subduction have been proposed as origins for these eclogites, geochemical study has demonstrated that these eclogites have protoliths of oceanic affinity (Song *et al.*, 2006; Chen *et al.*, 2009). In the future, it would be desirable to find coesite-bearing zircons for precise dating of the UH*P* metamorphism.

Acknowledgement: We are grateful to Drs C. Mattinson and C. Menold for their critical and constructive review of the manuscript. We thank C. Zhang (PKU) and F. Brink

(EMU, ANU) for their generous help with the laboratory work. This study was supported by the National Natural Science Foundation of China (Grants 40821002 and 40802016), China Postdoctoral Science Foundation funded project 200801028, Major State Basic Research Development Program (Grants 2009CB825007) and an ARC Discovery Grant to Ellis and Christy. The financial support by the 2008 Endeavour Australia Cheung Kong Research Fellowship granted to GBZ to undertake a Postdoctoral Research in ANU is gratefully acknowledged.

References

Carswell, D.A., O'Brien, P.J., Wilson, R.N., Zhai, M.G. (1997): Thermobarometry of phengite-bearing eclogites in the Dabie Mountains of Central China. *J. metamorphic Geol.*, **15**, 239–252.

Chen, D.L., Sun, Y., Liu, L., Zhang, A.D., Luo, J.H., Wang, Y. (2005): Metamorphic evolution of the Yuka eclogite in the North Qaidam, NW China: evidence from the compositional zonation of garnet and reaction texture in the rock. *Acta Petrol. Sin.*, **21**, 4, 1039–1048 (in Chinese with English abstract).

Chen, D.L., Liu, L., Sun, Y., Liou, J.G. (2009): Geochemistry and zircon U–Pb dating and its implications of the Yukahe HP/UHP terrane, the North Qaidam, NW China. *J. Asian Earth Sci.*, **35**, 232–244.

Chopin, C. (1984): Coesite and pure pyrope in high-grade blueschists of the western Alps: a first record and some consequences. *Contrib. Mineral. Petrol.*, **86**, 107–118.

Droop, G.R.T., (1987): A general equation for estimating Fe^{3+} microprobe analyses, using stoichiometric criteria. *Mineral. Mag.*, **51**, 431–435.

Evans, B. (2007): The Synthesis and Stability of Some End-Member Amphiboles. *Rev. Mineral. Geochem.*, **67**, 261–286.

Ferroir, T., Onozawa, T., Yagi, T., Merkel, S., Miyajima, N., Nishiyama, N., Irifune, T., Kikegawa, T. (2006): Equation of state and phase transition in $KAlSi_3O_8$ hollandite at high pressure. *Am. Mineral.*, **91**, 327–332.

Graham, C.M. & Powell, R. (1984): A garnet-hornblende geothermometer: calibration, testing and application to the Pelona Schist, Southern California. *J. metamorphic Geol.*, **2**, 13–31.

Hermann, J., O'Neill, H.S.C., Berry, A.J. (2005): Titanium solubility in olivine in the system TiO_2-MgO-SiO_2: no evidence for an ultra-deep origin of Ti-bearing olivine. *Contrib. Mineral. Petrol.*, **148**, 746–760.

Holland, T.J.B. (1980): The reaction albite = jadeite + quartz determined experimentally in the range 600–1200°C. *Am. Mineral.*, **65**, 125–134.

Hwang, S., Shen, P., Chu, H., Yui, T., Liou, J., Sobolev, N., Zhang, R., Shatsky, V., Zayachkovsk, A. (2004): Kokchetavite: a new potassium-feldspar polymorph from the Kokchetav ultrahigh-pressure terrane. *Contrib. Mineral. Petrol.*, **148**, 380–389.

Jahn, B.M. (1999): Sm–Nd isotope tracer study of UHP metamorphic rocks: implications for continental subduction and collisional tectonics. *Int. Geol. Rev.*, **41**, 859–885.

Kohn, M.J. & Spear, F. S. (1990): Two new geobarometers for garnet amphibolites, with applications to southeastern Vermont. *Am. Mineral.*, **75**, 89–96.

Kretz, R. (1983): Symbols for rock-forming minerals. *Am. Mineral.*, **68**, 277–279.

Leake, B.E., Woolley, A.R., Arps, C.E.S. Brich, W.D., Gilbert, M.C., Grice, J.D., Hawthorne, F.C., Kato, A., Kisch, H.J., Krivovichev, V.G., Linthout, K., Laird, J., Mandarino, J.A., Maresch, W.V., Nickel, E.H., Rock, N.M.S., Schumacher, J.C., Smith, D.C., Stephenson, C.N., Ungaretti, L., Whittaker, E.J.W., Guo, Y.Z. (1997): Nomenclature of amphiboles: report of the Subcommittee on amphiboles of the International Mineralogical Association, Commission on New Minerals and Mineral Names. *Eur. J. Mineral.*, **9**, 623–651.

Liou, J.G., Zhang, R.Y., Ernst, W.G., Rumble, D., Maruyama, S. (1998): High-pressure minerals from deeply subducted metamorphic rocks. *Rev. Mineral.*, **37**, 33–96.

Liou, J.G. & Zhang, R.Y. (2002): Ultrahigh-pressure metamorphic rocks: Encyclopedia of Physical sciences and technology (third edition), Tarzana, CA, Academia Press **17**, 227–244.

Liou, J.G., Tsujimori, T., Zhang, R.Y., Katayama, I., Maruyama, S. (2004): Global UHP metamorphism and continental subduction/collision: The Himalayan model. *Int. Geol. Rev.*, **46**, 1–27.

Liu, L., Che, Z.C., Wang, Y., Luo, J.H. Chen, D.L. (1999): The petrological characters and geotectonic setting of high-pressure metamorphic rock belts in Altun Mountains. *Acta Petrol. Sin.*, **15**, 57–64 (in Chinese with English abstract).

Liu, L.G. (1978): High pressure phase transformations of albite, jadeite and nepheline. *Earth Planet. Sci. Lett.*, **37**, 438–444.

Massonne, H.J. & Schreyer, W. (1987): Phengite geobarometry based on the limiting assemblage with K-feldspar, phlogopite, and Quartz. *Contrib. Mineral. Petrol.*, **96**, 219–214.

Mattinson, C.G., Menold, C.A., Zhang, J.X., Bird, D.K. (2007): High- and Ultrahigh-Pressure Metamorphism in the North Qaidam and South Altyn Terranes, Western China. *Int. Geol. Rev.*, **49**, 969–995.

Menold, C., Manning, C., Yin, A., Chen, X. (2007): Metamorphic Evolution, Mineral Chemistry and Thermobarometry of Ultrahigh-Pressure Eclogites from the North Qaidam Metamorphic Belt, Western China. *Eos Trans. AGU*, **88**, 52, Fall Meet. Suppl., Abstract.

Menold, C., Manning, C., Yin, A., Tropper, P., Chen, XH., Wang, XF. (2009): Metamorphic evolution, mineral chemistry and thermobarometry of orthogneiss hosting ultrahigh-pressure eclogites in the North Qaidam metamorphic belt, Western China. *J. Asian Earth Sci.*, **35**, 273–284.

Page, F.Z., Essene, E.J., Mukasa, S.B. (2005): Quartz exsolution in clinopyroxene is not proof of ultrahigh pressures: evidence in the eclogites from the Eastern Blue Ridge, Southern Appalachians, USA. *Am. Mineral.*, **90**, 1092–1099.

Ravna, E.J.K. & Terry, M.P. (2004): Geothermobarometry of UHP and HP eclogites and schists – an evaluation of equilibria among garnet-clinopyroxene- kyanite-phengite-coesite/quartz. *J. metamorphic Geol.*, **22**, 579–592.

Schmädicke, E. (1991): Quartz pseudomorphs after coesite in eclogites from the Saxonian Erzgebirge. *Eur. J. Mineral.*, **3**, 231–238.

Smith, D.C. (1984): Coesite in clinopyroxene in the Caledonides and its implications for geodynamics. *Nature*, **310**, 641–644.

Smith, D.C. (2005): The SHAND quaternary system for evaluating the supersilicic or subsilicic crystal-chemistry of eclogite minerals, and potential new UHPM pyroxene and garnet end-members. *Mineral. Petrol.*, **88**, 87–122.

Song, S.G. (2001): Petrology, mineralogy and metamorphic evolution of the Dulan UH*P* Terrane in North Qaidam, NW China and its tectonic implications. Doctoral thesis in Institute of Geology, Chinese Academy of Geological Sciences.

Song, S.G., Yang, J.S., Xu, Z.Q., Liou, J.G., Shi, R.D. (2003a): Metamorphic evolution of the coesite-bearing ultrahigh-pressure terrane in the North Qaidam, northern Tibet, NW China. *J. metamorphic Geol.*, **21**, 631–644.

Song, S.G., Yang, J.S., Liou, J.G., Wu, C.L., Shi, R.D., Xu, Z.Q. (2003b): Petrology, geochemistry and isotopic ages of eclogites from the Dulan UH*P*M terrane, the North Qaidam, NW China. *Lithos*, **70**, 195–211.

Song, S.G., Zhang, L.F., Niu, Y.L. (2004): Ultra-deep origin of garnet peridotite from the North Qaidam ultrahigh-pressure belt, Northern Tibetan Plateau, NW China. *Am. Mineral.*, **89**, 1330–1336.

Song, S.G., Zhang, L.F., Chen, J., Liou, J.G., Niu, Y.L. (2005a): Sodic amphibole exsolutions in garnet from garnet-peridotite, North Qaidam UH*P*M belt, NW China: implications for ultra-deep-origin and hydroxyl defects in mantle garnets. *Am. Mineral.*, **90**, 814–820.

Song, S.G., Zhang, L.F., Niu, Y.L., Su, L., Jian, P., Liu, D.Y. (2005b): Geochronology of diamond-bearing zircons from garnet-peridotite in the North Qaidam UH*P*M belt, North Tibetan Plateau: A record of complex histories from oceanic lithosphere subduction to continental collision. *Earth Planet. Sci. Lett.* **234**, 99–118.

Song, S.G., Zhang, L.F., Niu, Y.L., Su, L., Song, B., Liu, D.Y. (2006): Evolution from oceanic subduction to continental collision: A case study of the Northern Tibetan Plateau inferred from geochemical and geochronological data. *J. Petrol.*, **47**, 435–455.

Song, S.G., Niu, Y.L., Zhang, L.F., Wei, C.J., Liou, J.G. (2009): Tectonic evolution of early Paleozoic HP metamorphic rocks in the North Qilian Mountains, NW China: New perspectives. *J. Asian Earth Sci.*, **35**, 334–353.

Yagi, A., Suzuki, T., Akogi, M. (1994): High Pressure transitions in the system $KAlSi_3O_8$-$NaAlSi_3O_8$. *Phys. Chem. Minerals*, **21**, 12–17.

Yang, J.J. & Deng, J.F. (1994): Garnet peridotites and eclogites in the northern Qaidam Mountains, Tibetan plateau: a first record. First Workshop on UH*P* Metamorphism and Tectonics, ILP Task Group III-6, Stanford, A-20.

Yang, J.J., & Powell, R. (2008): Ultrahigh-pressure garnet peridotites from the devolatilization of sea-floor hydrated ultramafic rocks. *J. metamorphic Geol.*, **26**, 695–716.

Yang, J.J. & Smith, D.C. (1989): Evidence for a former sanidine coesite-eclogite at Lanshantou, Eastern China, and the recognition of the Chinese Su-Lu Coesite-eclogite Province. *Terra Abstracts*, **1**, 26.

Yang, J.J., Godard, G., Smith, D.C. (1998): K-feldspar-bearing coesite pseudomorphs in an eclogite from Lanshantou (Eastern China). *Eur. J. Mineral.*, **10**, 969–985.

Yang, J.S., Xu, Z.Q., Song, S.G., Zhang, J.X., Wu, C.L., Shi, R.D., Li, H.B., Brunel, M. (2001): Discovery of coesite in the North Qaidam Early Palaeozoic ultrahigh pressure metamorphic belt, NW China. *C. R. Acad. Sci., Paris, Sciences de la Terre et des Planetes*, **333**, 719–724.

Yin, A. & Harrison, T.M. (2000): Geologic evolution of the Himalayan – Tibetan orogen. *Ann. Rev. Earth Planet Sci.*, **28**, 211–280.

Yin, A., Rumelhart, P., Butler, R., Cowgill, E., Harrison, T., Foster, D., Ingersoll, R., Zhang, Q., Zhou, X., Wang, X., Hanson, A., Raza, A. (2002): Tectonic history of the Altyn Tagh fault system in northern Tibet inferred from Cenozoic sedimentation. *Geol. Soc. Am. Bulletin*, **114**, 1257–1295.

Zhang, G.B., Song, S.G., Zhang, L.F., Niu, Y.L. (2008): The subducted oceanic crust within continental-type UH*P* metamorphic belt in the North Qaidam, NW China: Evidence from petrology, geochemistry and geochronology. *Lithos*, **104**, 99–118.

Zhang, G.B., Zhang, L.F., Song, S.G., Niu, Y.L. (2009a): UH*P* metamorphic evolution and SHRIMP geochronology of a coesite-bearing meta-ophiolitic gabbro in the North Qaidam, NW China. *J. Asian Earth Sci.*, **35**, 310–322.

Zhang, J.X., Zhang, Z.M., Xu, Z.Q., Yang, J.S., Cui, J.W. (2001): Petrology and geochronology of eclogites from the western segment of the Altyn Tagh, northwestern China. *Lithos*, **56**, 189–208.

Zhang, J.X., Meng, F.C., Yang, J.S. (2004): Eclogitic metapelites in the western segment of the north Qaidam Mountains: Evidence on ''in situ'' relationship between eclogite and its country rocks. *Sci. China Ser. D-Earth Sci.*, **12**, 1102–1112.

Zhang, J.X., Yang, J.S., Mattinson, C.G., Xu, Z.Q., Meng, F.C., Shi, R.D. (2005): Two contrasting eclogite cooling histories, North Qaidam H*P*/UH*P* terrane, western China: Petrological and isotopic constraints. *Lithos*, **84**, 51–76.

Zhang, J.X., Meng, F.C., Li, J.P., Mattinson, C.G. (2009b): Coesite in eclogite from the North Qaidam and its implications. *Chin. Sci. Bull.*, **54**, 1105–1110.

Zhang, L.F., Ellis, D.J., Jiang, W.B. (2002a): Ultrahigh pressure metamorphism in western Tianshan, China, part I: evidences from the inclusion of coesite pseudomorphs in garnet and quartz exsolution lamellae in omphacite in eclogites. *Am. Mineral.*, **87**, 853–860.

Zhang, L.F., Ellis, D., Williams, S., Jiang, W.B. (2002b): Ultrahigh pressure metamorphism in western Tianshan, China, part II: evidence from magnesite in eclogite. *Am. Mineral.*, **87**, 861–866.

Zhang, L.F., Ai, Y.L., Song, S.G., Song, B., Rubatto, D., Williams, S., Liou, J.G., Ellis, D. (2007): Triassic collision of Western Tianshan orogenic belt, China: evidences from SHRIMP U-Pb dating of zircon from eclogitic rocks. *Lithos*, **96**, 266–280.

Zhang, R.Y., Liou, J.G., Iizuka, Y., Yang, J.S. (2009c): First record of K-cymrite in North Qaidam UH*P* eclogite, Western China. *Am. Mineral.*, **94**, 222–228.

Zheng, Y.F., Fu, B., Gong, B., Li, L. (2003): Stable isotope geochemistry of ultrahigh-pressure metamorphic rocks from the Dabie-Sulu orogen in China: Implications for geodynamics and fluid regime. *Earth-Sci. Rev.*, **62**, 105–161.

Received 20 January 2009
Modified version received 26 May 2009
Accepted 22 September 2009